

Clustering of Photometric Luminous Red Galaxies II: Cosmological Implications from the Baryon Acoustic Scale

A. Carnero¹, E. Sánchez^{1*}, M. Crocce², A. Cabré³, E. Gaztañaga²

¹Centro de Investigaciones Enérgéticas, Medioambientales y Tecnológicas (CIEMAT), Madrid, Spain

²Institut de Ciències de l'Espai (IEEC-CSIC), Barcelona, Spain

³University of Pennsylvania, Philadelphia, USA

20 January 2013

ABSTRACT

A new determination of the sound horizon scale in angular coordinates is presented. It makes use of $\sim 0.6 \times 10^6$ Luminous Red Galaxies, selected from the Sloan Digital Sky Survey imaging data, with photometric redshifts. The analysis covers a redshift interval that goes from $z = 0.5$ to $z = 0.6$. We find evidence of the Baryon Acoustic Oscillations (BAO) signal at the $\sim 2.3\sigma$ confidence level, with a value of $\theta_{BAO}(z = 0.55) = (3.90 \pm 0.38)^\circ$, including systematic errors. To our understanding, this is the first direct measurement of the angular BAO scale in the galaxy distribution, and it is in agreement with previous BAO measurements. We also show how radial determinations of the BAO scale can break the degeneracy in the measurement of cosmological parameters when they are combined with BAO angular measurements. The result is also in good agreement with the WMAP7 best-fit cosmology. We obtain a value of $w_0 = -1.03 \pm 0.16$ for the equation of state parameter of the dark energy, or $\Omega_M = 0.26 \pm 0.04$ for the matter density, when the other parameters are fixed. We have also tested the sensitivity of current BAO measurements to a time varying dark energy equation of state, finding $w_a = 0.06 \pm 0.22$ if we fix all the other parameters to the WMAP7 best-fit cosmology.

Key words: data analysis – cosmological parameters – dark energy – large-scale structure of the universe

1 INTRODUCTION

The Baryon Acoustic Oscillations (BAO) signal imprinted in the galaxy distribution was first convincingly detected in 2005 (Eisenstein et al. 2005), using the Sloan Digital Sky Survey (SDSS)¹ data (York et al. 2000). Since then, several more detections at different redshifts intervals have been done (Percival et al. 2007; Sánchez et al. 2009; Gaztañaga et al. 2009; Reid et al. 2010; Percival et al. 2010; Kazin et al. 2010). All those used spectroscopic data in order to calculate galaxy redshifts, which has been the traditional technique to estimate distances, and measure the cosmological parameters through an averaged three-dimensional evaluation of the BAO scale.

Furthermore, the purely radial BAO signal was first obtained in Gaztañaga et al. (2009), where they measure the redshift intervals that correspond to the sound horizon scale at two different redshifts. There are ongoing or pro-

posed projects like BOSS (Schlegel et al. 2007) or BigBOSS (Schlegel et al. 2009) that will use massive measurements of galaxy spectra to obtain new measurements of the BAO scale, more precise and deeper than current determinations.

The feasibility of measuring the BAO signal using photometric redshifts (photoz) was first demonstrated in Padmanabhan et al. (2007) (see also Blake et al. (2007) and Thomas et al. (2011)). Large multiband imaging surveys are a powerful way to explore the clustering properties of galaxies. Their advantage is the possibility of mapping wider areas in deeper volumes, compared with spectroscopic surveys. However, the precision of the photoz is worse than its spectroscopic counterpart. There are projects like DES (The Dark Energy Survey Collaboration 2005), PanSTARRS (Kaiser et al. 2000) or LSST (Tyson et al. 2003) that aim to obtain the most precise cosmological constraints using imaging alone, compensating the lack of precision in redshift, with a larger volume and higher galaxy density, and also with the possibility of studying different galaxy populations.

* E-mail:eusebio.sanchez@ciemat.es

¹ <http://www.sdss.org>

In this paper, a new determination of the BAO angular

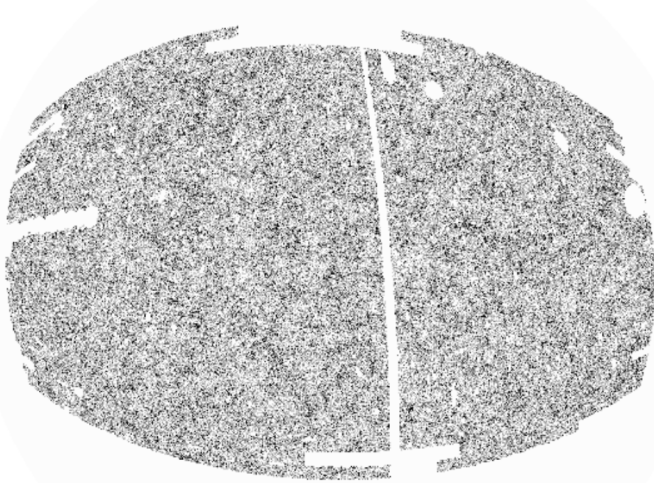


Figure 1. The mask used in this analysis, as a Mollweide projection in equatorial coordinates. The white regions are excluded of the analysis. The vertical band is due to the photoz used in this analysis.

scale is presented. The measurement has been done upon a photometric sample of Luminous Red Galaxies (LRG), obtained from the SDSS seventh data release (DR7), published by Abazajian et al. (2009). We study the BAO signal at a redshift interval that goes from $z = 0.5$ to $z = 0.6$, using the photometric sample described in the companion paper (Crocce et al. 2011). This measurement is the first direct detection of the purely angular BAO signal, and it is complementary to the purely radial BAO and to the three-dimensional averaged BAO signal, contributing to break degeneracies in the determination of cosmological parameters.

We use a model independent method to measure the angular BAO scale with precision (Sánchez et al. 2011). The method is based on a parameterization of the angular correlation function as a sum of a power law, a constant and a Gaussian. There are a total of 6 parameters and the BAO position and its significance are given by the location and S/N in amplitude of the Gaussian. It is robust against systematic errors, it uses only observable quantities and it is independent of any assumption about other parameters or the shape of the correlation function. Furthermore, we have evaluated the systematic errors associated with the measurement.

The paper is organized as follows. First, we briefly explain the LRG selection criteria, that is common with the companion paper (Crocce et al. 2011). Then, the measurement of the angular BAO scale in the 2-pt angular correlation function is discussed. Next, we combine this result with previous measurements of the averaged and radial BAO scales to obtain new cosmological constraints, and finally, we comment on the conclusions.

2 SELECTION OF THE GALAXY SAMPLE

We perform a color based selection of LRG in the SDSS-DR7 imaging sample, based on that published by Cabré et al. (2006). The selection is described in more detail in the companion paper (Crocce et al. 2011). First, we select the region

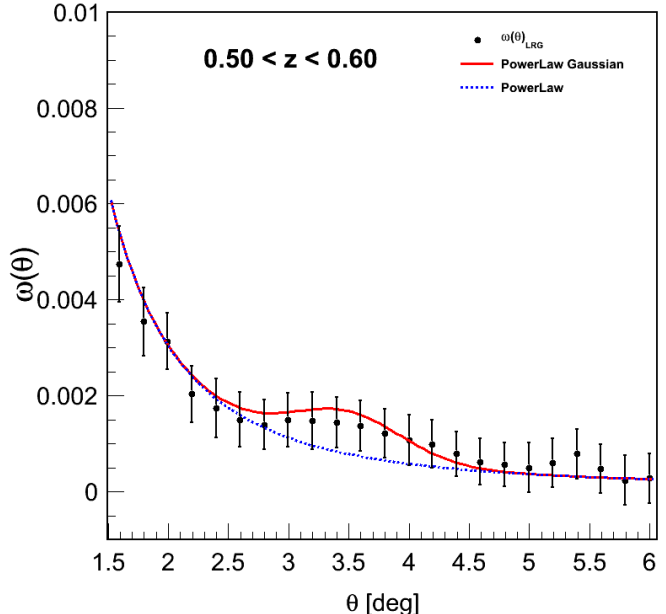


Figure 2. The observed angular correlation function for the analyzed redshift bin, $\omega(\theta, z = 0.55)$. The solid line is the result of fitting the function to a power law plus a Gaussian, following the method presented in Sánchez et al. (2011), and including the covariance matrix. The dotted line shows only the power law. The BAO signal is detected with a statistical significance of 2.3σ .

in the color–color space that is populated by LRGs (Eisenstein et al. 2001), requiring $(r-i) > \frac{(g-r)}{4} + 0.36$ and $(g-r) > -0.72 (r-i) + 1.7$. Then, we minimize the star contamination, imposing an additional set of cuts: $17 < r_{Petro} < 21$, $0 < \sigma_{r_{Petro}} < 0.5$, $0 < (r-i) < 2$, $0 < (g-r) < 3$ and $22 \text{ mag arcsec}^{-2} < \mu_{50} < 24.5 \text{ mag arcsec}^{-2}$. In these cuts, g , r and i are the model magnitudes corrected by extinction, $\sigma_{r_{Petro}}$ is the error on the Petrosian magnitude r_{Petro} and μ_{50} is the mean surface brightness within the Petrosian half-light radius in the r band. Finally, only galactic latitudes $b > 25^\circ$ are considered. A total of $\sim 1.5 \times 10^6$ objects are selected, with a star contamination of $4 \pm 1\%$, determined using the spectroscopic SDSS sample.

We use the angular mask depicted in Figure 1 as a Mollweide projection in equatorial coordinates, which amounts a total area of 7136 square degrees. Only the largest contiguous area of the survey is considered in this analysis. There is also a vertical band in the mask that it is excluded due to the photoz catalog we have used, described in the next section. For further details, see Crocce et al. (2011).

3 CORRELATION FUNCTIONS

The photometric redshift determination developed in Oyaito et al. (2008) is used in this analysis. It is combined with the value added catalog of Cunha et al. (2009), where the photometric redshift probability distribution function (PDF) for every object is given, following the method of Lima et al. (2008). We determine the redshift for each object as the maximum of its PDF, but the full PDF distribution is used to estimate the true distribution of objects

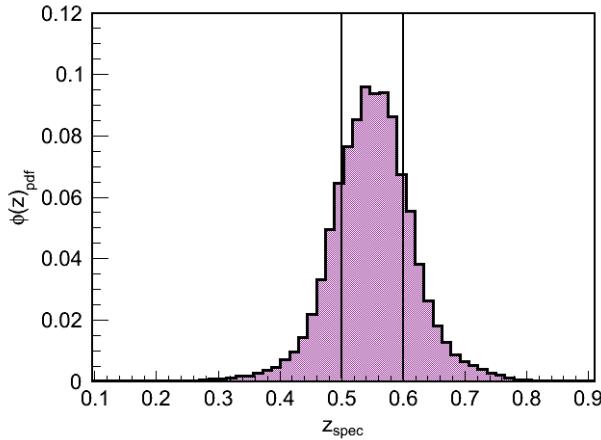


Figure 3. The true redshift distribution of selected galaxies. It has been obtained summing all the galaxies PDFs within the bin. The vertical lines are the limits of the photometric redshift bin under study.

with redshift. Objects with PDF distributions that do not satisfy good quality requirements are rejected (see Crocce et al. (2011) for a detailed description of the photometric redshift quality requirements). The highest redshift region, $0.5 < z < 0.6$, is chosen for this analysis. It contains 0.61×10^6 objects.

We chose this bin width for two reasons. First, a much narrower bin does not enhance the sensitivity, due to the dilution effect caused by the photoz. And second, a much wider bin will decrease the amplitude of the correlation function, making more difficult to detect the BAO signal.

Figure 2 shows the measured angular correlation function (dots) in this redshift bin. It has been computed using the Landy & Szalay estimator (Landy & Szalay 1993).

The error and covariances in the angular correlation function have been evaluated using three independent methods. First, we have generated 50 artificial realizations of the observed $\omega(\theta)$. The error is computed as the dispersion of the generated realizations, taking into account the fraction of the sky that the survey covers. Second, we have used the standard Jack-Knife procedure, dividing the area in 80 regions. And third, we have used the theoretical description, following the result in Crocce et al. (2010). The three determinations agree within 25% in the square-root of the diagonal elements of the covariance matrix. To see a more detailed discussion of the error calculation, see Crocce et al. (2011).

4 RESULTS

We use the method described in Sánchez et al. (2011) to measure the BAO scale, using the observed correlation function of the previous section. The method is based on the description of $\omega(\theta)$ as the sum of a power law to describe the continuum and a Gaussian peak to describe the BAO feature:

$$\omega(\theta) = A + B\theta^\gamma + C e^{-(\theta-\theta_{FIT})^2/2\sigma^2} \quad (1)$$

This expression is fitted to the data with free parameters $A, B, C, \gamma, \theta_{FIT}$ and σ . The true BAO scale is recovered from the fitted parameter θ_{FIT} after correcting for the projection effect due to the width of the redshift bin where the analysis is performed:

$$\theta_{BAO} = \alpha(z, \Delta z) \theta_{FIT}. \quad (2)$$

The factor α is taken from the analysis presented in Sánchez et al. (2011), and depends on the redshift, z , and the redshift bin width, Δz .

The fit is presented in Figure 2 (solid line), compared to a single power law (dotted line). This fit includes the full covariance matrix, obtained with the Jack-Knife method, as seen in the companion paper. In Crocce et al. (2011) we calculate both the Jack-Knife and the analytical covariances, finding that both are compatible with each other and that results don't depend on the chosen covariance matrix (Crocce et al. 2011).

The BAO peak is detected with a statistical significance of 2.3 standard deviations. The statistical significance is computed using two methods. First, we use the fitted parameter C from Equation 1, and we quote the significance as its difference from zero. Second, we compare the result with a theoretical model that includes the BAO wiggles and with a model that doesn't include them (this comparison is fully described in Crocce et al. (2011)). Both determinations agree in the significance of the detection.

4.1 Systematic Errors

The main systematic errors affecting this measurement have been described in Sánchez et al. (2011), and we add them to our error budget here, except for the photometric redshift, which is recalibrated. The reason for this recalibration is that the photometric redshift in SDSS is not perfectly Gaussian, as it was supposed in Sánchez et al. (2011).

We have recalibrated the photoz error by calculating the dispersion in the BAO scale if we compute $\omega(\theta)$ with different photoz codes, all contained in the SDSS DR7 catalog. We redo the full analysis using the photometric redshift given by the *photozd1* and also by using the full PDF as the redshift, and not only the maximum probability. In the latter case, all galaxies has a probability to lay within the selected redshift bin, for example, in the redshift bin $0.5 \leq z \leq 0.6$. The only difference in the numerical algorithm is that, instead of calculating distances between pairs of galaxies, now we calculate distances between probabilities of galaxies, and weight the distance depending on the probability of pairs in the given bin.

We found that the amplitude of the correlation function does change, being smoother if we use the full PDF, but the measured scale θ_{BAO} is stable within 2% for all cases, including the *photozd1* estimation. Therefore, we add a contribution of 2%, coming from the different photoz code used, to the 5% found in Sánchez et al. (2011), which only accounts for the smearing of the photoz in a ideal Gaussian case. The total systematic error due to photometric redshift is then $\Delta\theta_{BAO}(\text{photoz}) = 7\%$.

Moreover, there are some additional effects that need to be taken into account on top of those of Sánchez et al.

(2011). These are the effects related to the selection of the sample (selection cuts, mask and contamination).

To evaluate the systematic error associated to the selection criterias, we vary the selection cuts of section 2 and recompute $\omega(\theta)$. Then, we compare the new measured θ_{BAO} with the nominal value. We have tested variations in μ_{50} , $(r - i)$ and $(g - r)$ within 10% of their nominal limits in section 2. The maximum variation found is $\Delta\theta_{BAO}(\text{selection}) = 2.5\%$, when we vary the μ_{50} limits. In all cases, variations in θ_{BAO} are always below the statistical uncertainty, that in our case is $\sim 5\%$. $\Delta\theta_{BAO}(\text{selection}) = 2.5\%$ is assigned as the systematic error due to the sample selection. This is actually likely to be conservative and most likely larger than the true 1σ value, but it is almost negligible compared to the 7% uncertainty of the photoz and the 5% statistical uncertainty.

We have also varied the mask in order to assess further uncertainties in our result. First we relax the cut in $b > 25^\circ$, and allow areas with $b < 25^\circ$. The effect of this cut in the galaxy number density can be seen in Figure 3 of the companion paper Crocce et al. (2011). There is a gradient in the number density of galaxies at low galactic latitudes, implying there is a population of objects, belonging to our galaxy, that is contaminating the sample. The effect in θ_{BAO} is similar to the effect that we obtain when we vary the galaxy selection cuts. Both produce smooth distortions in the clustering signal.

We also compute $\omega(\theta)$ for different quality values of extinction, seen at the bottom panel of Figure 4 in the companion paper Crocce et al. (2011). We eliminate areas with extinction higher than 0.15, 0.2 and without limits. Variations in θ_{BAO} are almost negligible, as we are dominated by the statistical error. For the mask, the strongest difference occurs if we allow areas with $b > 20^\circ$. The variation is of the 2%, associated with the mask systematic error as $\Delta\theta_{BAO}(\text{mask}) = 2\%$.

We recall that both error estimations are likely to be overestimated, although both are almost negligible in comparison with the statistical error of 5% and the 7% photoz systematic error, therefore, and considering the level of precision in the data, we believe it is reasonable to follow this prescription.

The influence of stars contamination has also been checked. We have fitted the correlation function including the star contamination as a constant factor, multiplied by the star correlation function (see Crocce et al. (2011)). The influence is found to be negligible, since the correlation function of stars varies very slowly with the angular scale. Variations in θ_{BAO} are $\Delta\theta_{BAO}(\text{stars}) < 0.1\%$. Moreover, we have included different levels of stars contamination in the theoretical correlation functions presented in Sánchez et al. (2011), always as a constant factor multiplied by the star correlation function. We have applied our method to all of them and we found that the θ_{BAO} obtained with our parameterization is insensitive to the presence of stars, at least for contaminations up to 10%.

The full accounting of systematic errors is presented in Table 1. The total systematic error budget is $\Delta\theta_{BAO}(\text{sys}) = 8.0\%$.

About the significance of the detection, we found that the effect of these systematics in the significance can produces maximum changes of the order of the 10%, up to a

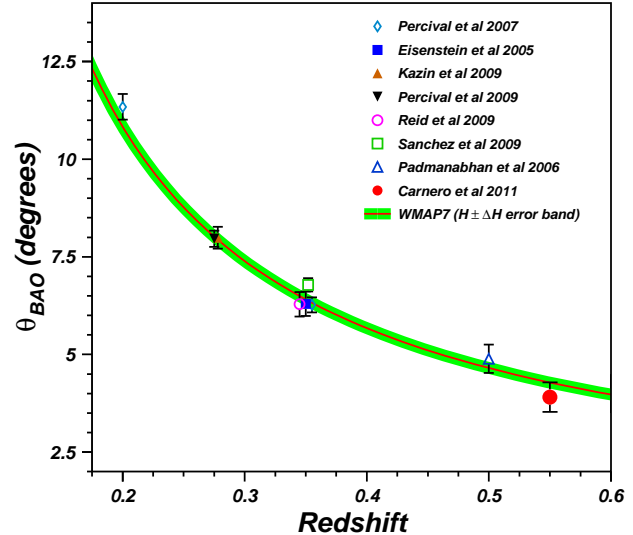


Figure 4. The angular BAO scale as a function of redshift. The measurement presented in this paper is the solid dot. Its error includes both the statistical and the systematic contributions. The other measurements are inferred from the given reference by translating the three-dimensional averaged distance parameter D_V , into an angular scale, with the fiducial cosmology used in each reference. All of them are compatible with the WMAP7 cosmology (solid line). The band includes the uncertainty in the Hubble constant H_0 . Some of the measurements at $z = 0.35$ have been slightly displaced in redshift for clarity.

Systematic error	$\Delta\theta_{BAO}$
Parameterization	1%
Photometric redshift error	7%
Redshift space distortions	1%
Theory	1%
Projection effect	1%
Selection of the Sample	2.5%
Survey mask	2%

Table 1. Estimation of systematic errors in the determination of θ_{BAO} . Those above the horizontal line are taken from Sánchez et al. (2011), except the error coming from the photometric redshift, which has been recalibrated for this work. The others are the main new contributions that arise from a real photometric redshift survey.

significance of 2.6σ , if we cut in $b > 20^\circ$ and using the maximum probability as the redshift and the nominal color cuts. We don't find any clear correlation with cuts or with which photoz code we used. This is due to the fact that we are yet limited by statistical uncertainties and the smearing of the photoz.

4.2 Comparison with Previous Measurements

The fitted angular scale, associated with the BAO scale is $\theta_{FIT}(z = 0.55) = 3.48 \pm 0.19^\circ$, obtained upon a redshift bin of width $\Delta z_{photo} = 0.1$. Following Sánchez et al. (2011), this value must be corrected to obtain the true BAO angular scale, $\theta_{BAO} = \alpha(z, \Delta z)\theta_{FIT}$. For this redshift and bin width,

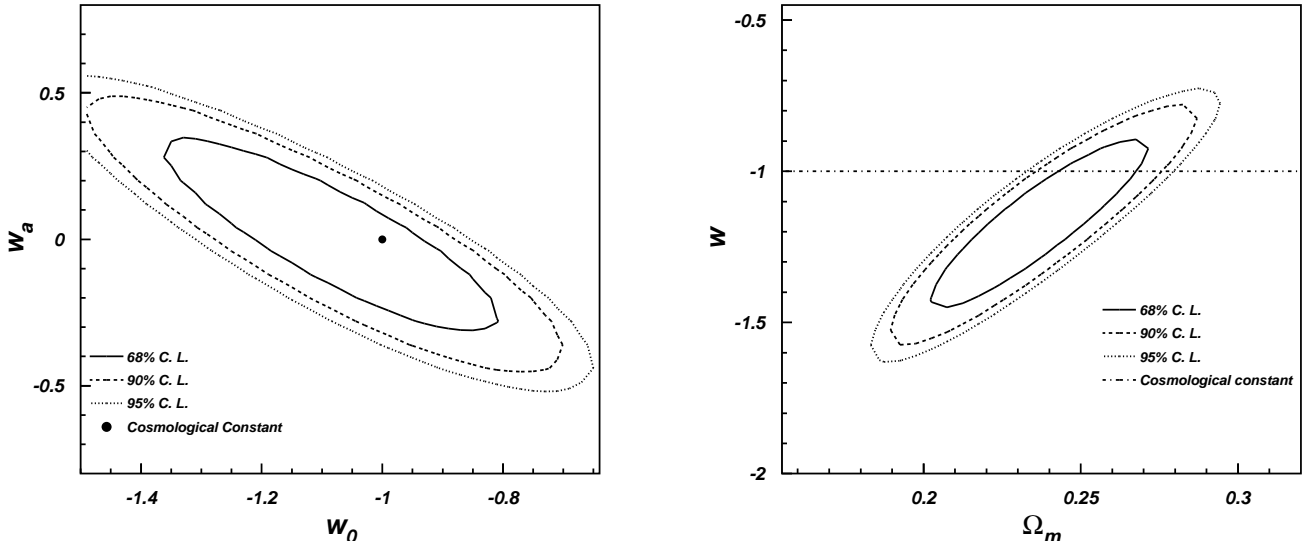


Figure 5. Constraints in the equation of state of the dark energy using the data in Figure 4 and the radial BAO measurements from Gaztañaga et al. (2009). Left: Constraints in the plane w_0 , w_a , where $w(a) = w_0 + w_a(1 - a)$, and a the scale factor of the universe. Data is compatible with a dark energy that behaves as a cosmological constant to better than 1σ . (solid dot). Right: Constraints in the plane w , Ω_m . The dash-dotted line corresponds to the Cosmological Constant and is compatible with the data.

the correction is $\alpha(z = 0.55, \Delta z_{true} = \sqrt{2\pi}\Delta z_{photo}) = 1.12$. The final result for the BAO scale, including statistical and systematic errors is $\theta_{BAO}(z = 0.55) = 3.90 \pm 0.38^\circ$.

The evolution of the angular BAO scale with redshift is presented in Figure 4. The measurement presented in this analysis is the solid dot, including the statistical and the systematic errors. The other measurements are inferred from the given reference, by translating the three-dimensional averaged distance parameter D_V into an angular scale, with the fiducial cosmology used in each reference. All the measurements are in agreement with the WMAP7 cosmology to better than 1σ , represented by the solid line. The band includes the uncertainty in the determination of the Hubble constant H_0 (Riess et al. 2011).

We have tested the sensitivity of current BAO measurements to a dark energy with an equation of state parameter that varies with time, as $w(a) = w_0 + w_a(1 - a)$, where a is the scale factor of the universe. In Figure 5 (Left) we show the allowed regions for parameters w_0 and w_a , when we fit the evolution of the BAO scale using the data in Figure 4, plus the radial BAO scales at $z = 0.24$ and $z = 0.43$ from Gaztañaga et al. (2009), which values are $r_s(z = 0.24) = 110.3 \pm 2.9 \pm 1.8$ Mpc/h and $r_s(z = 0.43) = 108.9 \pm 3.9 \pm 2.1$ Mpc/h. We fix all the other cosmological parameters to their values in the WMAP7 w CDM cosmology (Komatsu et al. 2011), and we use the most recent Hubble constant determination (Riess et al. 2011). We have chosen the values of Percival et al. (2007) at $z = 0.20$, Percival et al. (2010) at $z = 0.275$, Sánchez et al. (2009) at $z = 0.35$ and the measurement presented in this paper at $z = 0.55$, since the other measurements at the same or similar redshifts are strongly correlated. Data is compatible at the 1σ level with a dark energy that behaves as a cosmological constant ($w_0 = -1$, $w_a = 0$, included as the solid dot in Figure 5).

We have also studied the sensitivity of current BAO measurements in the plane w , Ω_m , under the same conditions than above: we use the same data points and also include the radial BAOs. The other parameters remain fixed plus w_a , which is fixed to zero. The result is presented in Figure 5 (Right). The dash-dotted line shows the expected value for the Cosmological Constant, compatible with the data.

If we fit to a single parameter, it gives $w = -1.03 \pm 0.16$. The data is compatible with a cosmological constant with a precision of the $\sim 20\%$ in w . If we do the same study for Ω_M , we find a value of $\Omega_M = 0.26 \pm 0.04$. Both measurements include systematic errors, and have been obtained fixing all the other parameters to the same values than above, except H_0 , which has been varied within its uncertainty. We have now included the influence of H_0 because it is larger in this case. The error budget in the parameter becomes 40% larger, including the H_0 uncertainty. The influence in the previous 2-dimensional constraints is smaller.

The influence of our measurement in the cosmological constraints is shown in Figure 6 (Left), where we compare the constraints at 68% C. L. for all the data (bold) with the constraints obtained when the point of this study ($z = 0.55$) is excluded (light). The contribution of the new point is not negligible, since its inclusion makes the constraints more precise. In particular, the figure of merit, defined as the inverse of the area within contours improves by 5%. Moreover, we have studied how the angular and the radial BAO scale measurements contribute to the cosmological constraints. This is depicted in Figure 6 (Right), where the light vertical contour corresponds to the angular BAO scales and the light diagonal contour corresponds to the radial BAO scales. The bold contour are the full combination at 68% C. L., also presented in Figure 5 (Right). Both determinations are com-

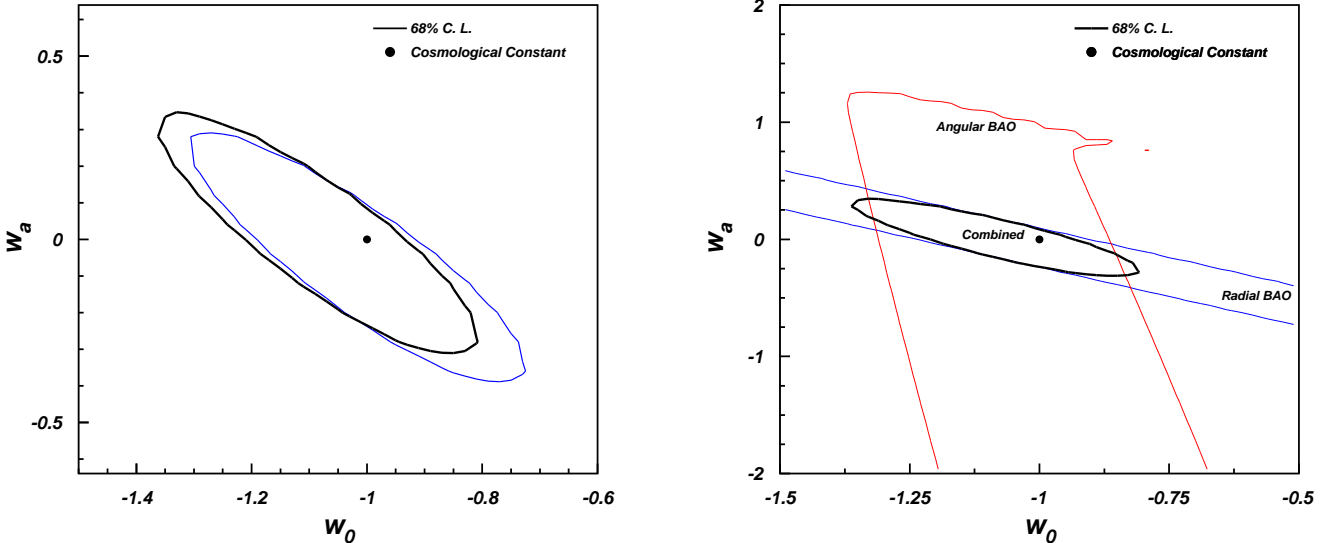


Figure 6. Left: The contribution of our determination $\theta_{BAO}(z = 0.55)$, to the dark energy equation of state constraints. The bold contour is the full combination, while the light contour is obtained when excluding our measurement at $z = 0.55$. The contribution of this new measurement is not negligible, improving by 5% the Figure of Merit. Right: Contribution to the cosmological constraints from the angular (light vertical contour) and radial (light diagonal contour) BAO scale measurements. Both determinations are complementary, and the combination (bold contour) breaks the degeneracy, making the constraints more precise.

plementary and the combination clearly breaks degeneracies between cosmological parameters, enhancing the sensitivity.

Some comments about the detection of the radial BAO are in order, since there are some claims saying that there is no convincing evidence of the detection (Kazin et al. 2010). For them, detection means a preference for a model with BAO as compare to a model without BAO. Nevertheless, we also consider the appreciation given in Cabré & Gaztañaga (2011), who argue that it is not justified to use any of the current BAO measurements (radial or not) to do a clear model selection. Instead, Cabré & Gaztañaga (2011) show that BAO measurements can be used for parameter fitting within CDM models, which is what we present here.

5 CONCLUSIONS

We have measured the BAO signal in the distribution of galaxies at the redshift interval $0.5 < z < 0.6$, using a LRG sample selected from the SDSS DR7 photometric catalog. The BAO signal is detected with a statistical significance of 2.3 standard deviations, as expected from the characteristics of the sample (Crocce et al. 2011). The result is in agreement with the WMAP7 cosmology, we find $\theta_{BAO}(z = 0.55) = (3.90 \pm 0.38)^\circ$ for the angular BAO scale, including systematic errors. This is the first direct measurement of the BAO signal in angular space, and complements previous three-dimensional averaged and radial BAO measurements, making a significant contribution to break degeneracies between cosmological parameters. Combining with previous BAO measurements, this translates into $\omega = -1.03 \pm 0.16$ for the equation of state parameter of the dark energy, and $\Omega_M = 0.26 \pm 0.04$ for the matter density.

Our relative error determination in the angular BAO scale is 9%. This is larger than the 6.5% uncertainty found by Padmanabhan et al. (2007), the only previous photometric determination of the BAO scale. This difference is not totally surprising, since our method to recover the BAO position only uses the information around the BAO peak, while Padmanabhan et al. (2007) includes all scales with $k > 0.3$. The impact and analysis of systematic effects is also quite different. For example, the above error in Padmanabhan does not include the photometric redshift uncertainties, while this effect dominates our systematic error budget (see Table1).

We have also studied the sensitivity of all BAO measurements obtained up to date, to a time varying dark energy equation of state, finding $\omega_a = 0.06 \pm 0.22$ when we fix all the other parameters to the WMAP7 cosmology. Therefore, the data is well described by a dark energy that behaves as a cosmological constant.

This study is a confirmation of the feasibility to obtain precise cosmological constraints using photometric redshift surveys. This allows wider and deeper galaxy samples, with the caveat of a less precise redshift. However, the smaller precision in the redshift determination is compensated with the higher statistics, allowing a precise measurements of cosmological parameters.

ACKNOWLEDGEMENTS

Funding for the SDSS and SDSS-II has been provided by the Alfred P. Sloan Foundation, the Participating Institutions, the National Science Foundation, the U.S. Department of Energy, the National Aeronautics and Space Administration, the Japanese Monbukagakusho, the Max Planck Soci-

ety, and the Higher Education Funding Council for England. The SDSS Web Site is <http://www.sdss.org/>.

The SDSS is managed by the Astrophysical Research Consortium for the Participating Institutions. The Participating Institutions are the American Museum of Natural History, Astrophysical Institute Potsdam, University of Basel, University of Cambridge, Case Western Reserve University, University of Chicago, Drexel University, Fermilab, the Institute for Advanced Study, the Japan Participation Group, Johns Hopkins University, the Joint Institute for Nuclear Astrophysics, the Kavli Institute for Particle Astrophysics and Cosmology, the Korean Scientist Group, the Chinese Academy of Sciences (LAMOST), Los Alamos National Laboratory, the Max-Planck-Institute for Astronomy (MPIA), the Max-Planck-Institute for Astrophysics (MPA), New Mexico State University, Ohio State University, University of Pittsburgh, University of Portsmouth, Princeton University, the United States Naval Observatory, and the University of Washington.

We thank the Spanish Ministry of Science and Innovation (MICINN) for funding support through grants AYA2009-13936-C06-01, AYA2009-13936-C06-03, AYA2009-13936-C06-04 and through the Consolider Ingenio-2010 program, under project CSD2007-00060.

We thank Carlos Cunha for his valuable comments about the photometric redshift.

REFERENCES

- Abazajian K. N., Adelman-McCarthy J. K., Agüeros M. A., Allam S. S., Allende Prieto C., An D., Anderson K. S. J., Anderson S. F., Annis J., Bahcall N. A., et al. 2009, ApJS, 182, 543
- Blake C., Collister A., Bridle S., Lahav O., 2007, MNRAS, 374, 1527
- Cabré A., Gaztañaga E., 2011, MNRAS, 412, 98
- Cabré A., Gaztañaga E., Manera M., Fosalba P., Castander F., 2006, MNRAS, 372, 23
- Crocce M., Cabre A., Gaztañaga E., 2010, ArXiv e-prints, 1004.4640 [astro-ph]
- Crocce M., et al., 2011, ArXiv e-prints, 1104.5236 [astro-ph]
- Cunha C. E., Lima M., Oyaizu H., Frieman J., Lin H., 2009, MNRAS, 396, 2379
- Eisenstein D. J., et al., 2001, AJ, 122, 2267
- Eisenstein D. J., et al., 2005, ApJ, 633, 560
- Gaztañaga E., A. C., Hui L., 2009, MNRAS, 399, 1663
- Kaiser N., Tonry J. L., Luppino G. A., 2000, PASP, 112, 768
- Kazin E. A., Blanton M. R., Scoccimarro R., McBride C. K., Berlind A. A., 2010, ApJ, 719, 1032
- Kazin E. A., et al., 2010, ApJ, 710, 1444
- Komatsu E., et al., 2011, ApJS, 192, 18
- Landy S. D., Szalay A. S., 1993, ApJ, 412, 64
- Lima M., Cunha C. E., Oyaizu H., Frieman J., Lin H., Sheldon E. S., 2008, MNRAS, 390, 118
- Oyaizu H., Lima M., Cunha C. E., Lin H., Frieman J., Sheldon E. S., 2008, ApJ, 674, 768
- Padmanabhan N., et al., 2007, MNRAS, 378, 852
- Percival W. J., Cole S., Eisenstein D. J., Nichol R. C., Peacock J. A., Pope A. C., Szalay A. S., 2007, MNRAS, 381, 1053
- Percival W. J., et al., 2010, MNRAS, 401, 2148
- Reid B. A., et al., 2010, MNRAS, 404, 60
- Riess A. G., et al., 2011, ApJ, 730, 119
- Sánchez A. G., Crocce M., Cabré A., Baugh C. M., Gaztañaga E., 2009, MNRAS, 400, 1643
- Sánchez E., et al., 2011, MNRAS, 411, 277
- Schlegel D. J., et al., 2007, in American Astronomical Society Meeting Abstracts Vol. 38 of Bulletin of the American Astronomical Society, SDSS-III: The Baryon Oscillation Spectroscopic Survey (BOSS). p. 132.29
- Schlegel D. J., et al., 2009, ArXiv e-prints, 0904.0468 [astro-ph]
- The Dark Energy Survey Collaboration 2005, ArXiv e-prints, astro-ph/0510346
- Thomas S. A., Abdalla F. B., Lahav O., 2011, MNRAS, 412, 1669
- Tyson J. A., Wittman D. M., Hennawi J. F., Spergel D. N., 2003, Nuclear Physics B Proceedings Supplements, 124, 21
- York D. G., et al., 2000, AJ, 120, 1579